JOURNAL OF AIRCRAFT
Vol. 48, No. 2, March–April 2011

Engineering Notes

Experimental Studies of Open Cavity Configurations at Transonic Speeds with Flow Control

C. Lada*
Delft University of Technology, 2629 HS Delft, The Netherlands
and
K. Kontis†
University of Manchester, Manchester, England M60 1QD, United Kingdom

DOI: 10.2514/1.C031174

Nomenclature

D	=	cavity depth, mm
f	=	frequency, Hz
L	=	cavity length, mm
M_∞	=	freestream Mach number
s	=	cell span
St	=	Strouhal number
U_∞	=	freestream velocity, m/s
X_c	=	position along cavity length, mm
α	=	empirical constant
γ	=	ratio of specific heat of test gas (taken to be equal to 1.4 for perfect gases)
κ	=	empirical constant

I. Introduction

CHANGES in mean static pressure distributions inside a cavity can result in large pressure gradients, and the unsteady flow disturbances can generate self-sustaining oscillations that, in turn, generate acoustic tones that radiate from the cavity. Both the steady and the unsteady flows can present difficulties for store separation from an internal weapons bay. The steady flows can generate large nose-up pitching moments, and the unsteady flows can induce structural vibration. To ensure safe carriage and separation for transonic and supersonic speeds, a better understanding of the physics of cavity flows must be obtained. Little research has been performed on closed cavities, and even less in transitional cavities. First, they occur less often because of the size of weapons. Second, there are more complex types of flow structure and problems regarding open cavities. Finally, the flow structure in cavities has in general been assumed as two-dimensional. So the closed cavity flow can be assumed as the same as flow over a backward-facing step followed by flow over a forward-facing step. Roshko [1], Krishnamurty [2], Rossiter [3], and Sarohia [4] are some of the early investigators that studied the resulting flowfield inside cavities.

Received 7 July 2010; revision received 22 November 2010; accepted for publication 22 November 2010.

*Postdoctoral Researcher, Faculty of Aerospace Engineering, CleanEra/Acoustic Remote Sensing, Kluyverweg 1.

†Professor, School of Mechanical, Aerospace, and Civil Engineering, Sackville Street. Associate Fellow AIAA.

Rossiter [3], in 1964, proposed a semiempirical formula for predicting the frequency peaks in high subsonic compressible flows over cavities with a length-to-depth ratio $L/D \geq 1$. Noting that the characteristic frequencies vary proportionally to U_∞ and inversely to L, he plotted the Strouhal numbers $St_n = f_n L/U_\infty$ against the flow Mach number for various cavity configurations. The result is that the mode frequencies lie on a specific family of curves satisfying the following equation:

$$St_n = \frac{\alpha - \gamma}{M_\infty + 1/\kappa} \quad \text{or} \quad f = \frac{U_\infty}{L}\frac{\alpha - \gamma}{M_\infty + 1/\kappa} \tag{1}$$

where n is an integer corresponding to the mode number.

Since then, numerous studies have been done on cavity flows at transonic and supersonic speeds investigating several issues, either theoretically or experimentally, such as pressure fluctuations [5–10] and cavity flowfield characteristics [11–16]. A major issue that occurred after the aerodynamics and the acoustics inside the cavities were understood was to control the cavity flows in order to eliminate or alleviate all the undesired phenomena. There are some interesting recent reviews by Colonius [17], who provided a summary of numerical simulations on active flow control of acoustic resonance, and by Cattafesta et al. [18], who reviewed the experimental work on the same field.

II. Experimental Setup

The experiments took place in the Plint TE25/A supersonic wind tunnel. The wind tunnel is a high-speed closed-return facility, with a maximum Mach number of 1.7. The cavity models are four cubic models designed to fit to the access window of the tunnel, with diameter 128 mm. The L/D ratios were chosen to be open two and six. The length of each is set to 90 mm. There are 33 static pressure tapings, 17 of them are located inside the cavity and 16 outside the cavity on the circular plate; the pressure tapings inside the cavity are placed in three lines parallel to each other and to the direction of the flow. The middle line of tapings is located in the centerline of the cavity. The upper and lower lines are located 24 and 40 mm from the centerline. The pressure tapings were of 1 mm internal bore. Four different wedge inserts at four different angles of 15, 30, 45, and 60° were manufactured for each cavity model. Average pressures inside and around the cavities were collected with SenSym part number ASDX015 pressure transducers (0 to 15 psi). The fluctuating pressures were obtained using Kulite pressure transducers. To reveal the less dominant modes present inside the cavities, the dominant mode was filtered from the signal using a Butterworth band stop filter implemented in MATLAB. This filter was adjusted for the specific results but generally covered the region of 2400 to 2600 Hz. The Butterworth filter was chosen over other possible alternatives (Chebyshev type 1 or 2, elliptic filter) due to its smooth roll off and linearity in the stop band. For each L/D, the pressure readings were taken at a freestream Mach number of 0.8. Oil flow technique was employed to visualize the surface flow inside and around the cavity using a mixture of titanium dioxide with linseed oil and silicon.

III. Results and Discussion

A. Cavity Without Flow Control

Figure 1 shows the pressure coefficient distribution on the cavity floor for $L/D = 2$ and 6. Higher pressure regions were measured at either end of each cavity; a low pressure region was obtained at $0.1 < X_c/L < 0.3$, which indicates a forward region of recirculation, and another one was observed at $0.3 < X_c/L < 0.7$. The $L/D = 6$ cavity exhibits larger pressures at the trailing edge. This is expected

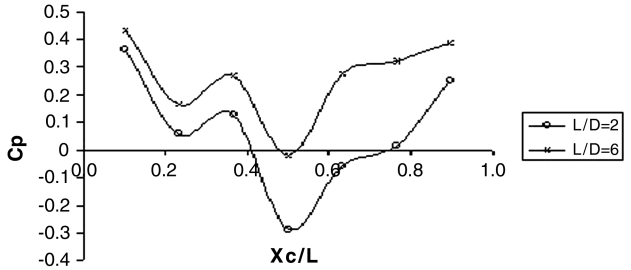

Fig. 1 Pressure distributions for cavities $L/D = 2$ and 6.

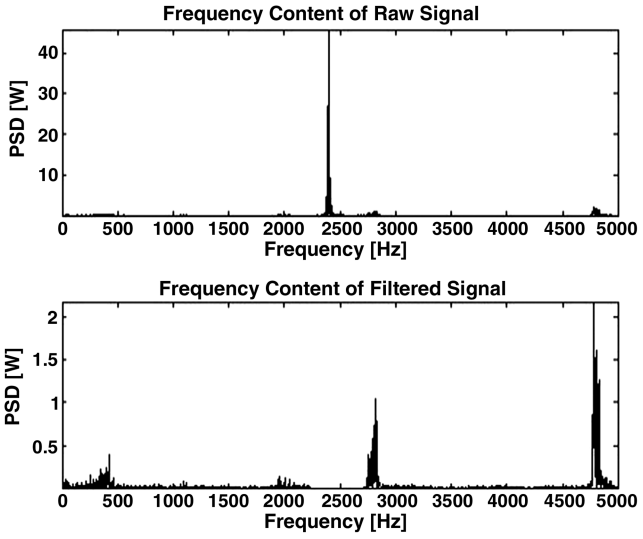

Fig. 2 Frequency content for cavity $L/D = 2$ without flow control.

since the $L/D = 6$ cavity is closer to the transitional type. Figure 2 shows the modes of resonance obtained in the filtered signal case for $L/D = 2$, with two additional peaks at roughly 450 and 2750 Hz. The large peak at 4750 Hz is a harmonic of the large peak at 2400 Hz. For the cavity $L/D = 6$, three strong peaks were identified in the spectrum. The first mode occurs at 750 Hz, the second mode occurs at 1750 Hz, and the third mode occurs at 3500 Hz.

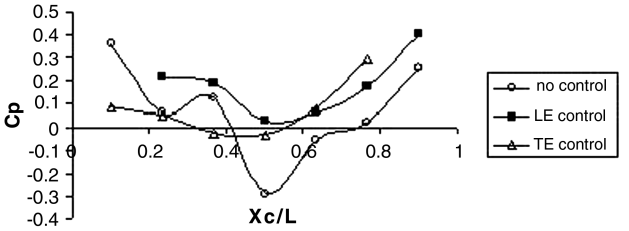

Fig. 4 Pressure distributions for cavity $L/D = 2$ with 15° wedge on leading edge (LE) or trailing edge (TE).

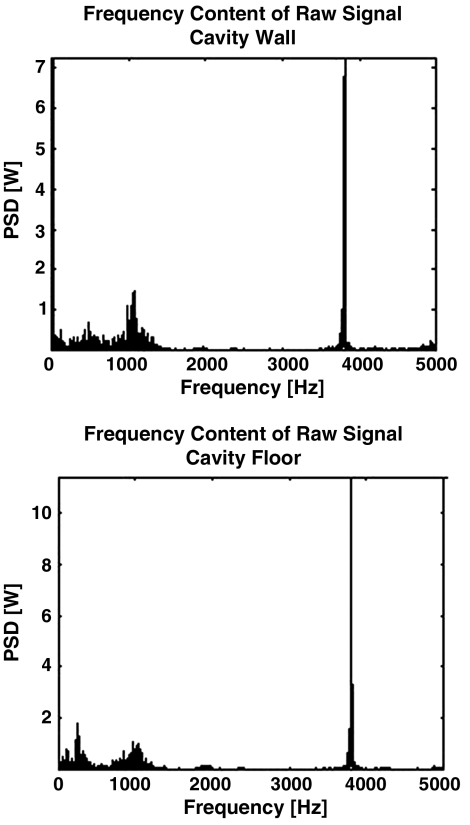

Fig. 5 Frequency content for cavity $L/D = 2$ with 15° wedge placed at the trailing edge.

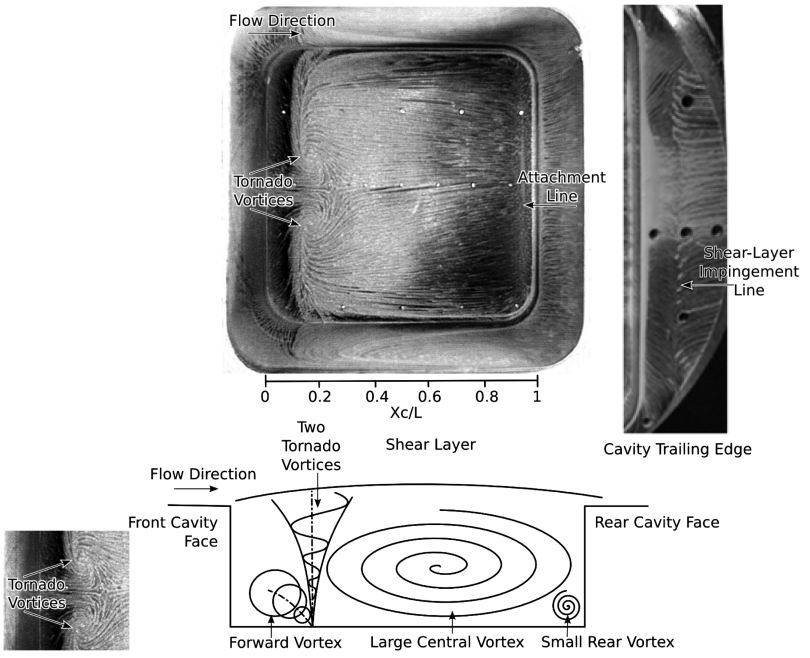

Fig. 3 Oil flow visualization for cavity $L/D = 2$ with a schematic of steady flow features and shear-layer impingement location at the cavity trailing edge.

The shear layer bridged the cavity $L/D = 2$ and attached aft of the trailing edge. The attachment line is shown in Fig. 3. Inside the cavity, there is an attachment line just before the trailing edge. A circulating flow is formed in the middle of the cavity. This is a large vortex and is the strongest vortex present. At $L/D = 2$, the flow accommodates two tornado vortices just after the leading edge of the cavity that are symmetric to the centerline, normal to and terminating on the cavity floor. These tornado vortices energize the forward vortex. Part of the shear layer enters the cavity and is divided into three streams. The central stream reinforces the large central vortex. The flow just outboard of the centerline follows the cavity floor, diverges laterally, and reinforces the forward tornado vortices. The flow even further outboard of the centerline follows the cavity floor upstream for a short distance, turns, and exits from the rear corners. As the cavity aspect ratio was increased to six, the two tornado vortices located just forward of the cavity leading edge in the $L/D = 2$ case are replaced by a separation line. This was expected, since no cellular structures are observed on cavities with $L/D > 2.2$ [15].

B. Cavity with Flow Control

By placing the 15° wedge at the leading edge of the $L/D = 2$ cavity at a Mach number of 0.8, the power of the second mode at 2500 Hz is increased greatly. The pressure distribution (Fig. 4) shows that there is an increase of pressure at the trailing edge of the cavity when the leading edge is tilted. This means that more energy is dissipated at the trailing edge of the cavity. The feedback loop is not disrupted, and the cavity tones are amplified. Placing the 15° wedge at the trailing edge of the cavity produced a much more beneficial effect. As is seen in Fig. 5, a large reduction of power spectral density (PSD) has been achieved across all modes; the dominant mode recorded on the cavity floor has been reduced dramatically from 320 to 5 W. The pressure results show that when the shear layer impinges

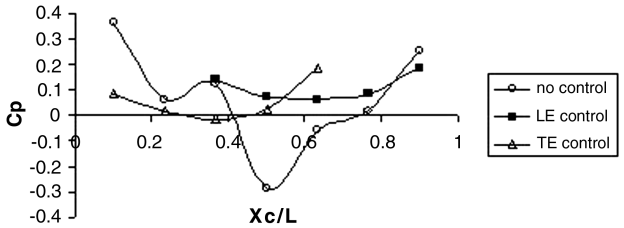

Fig. 6 Pressure distributions for cavity $L/D = 2$ with 30° wedge on leading or trailing edge.

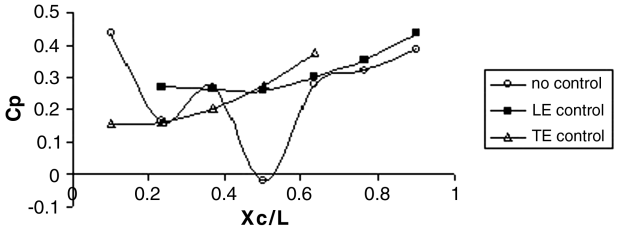

Fig. 8 Pressure distributions for cavity $L/D = 6$ with 15° wedge on leading or trailing edge.

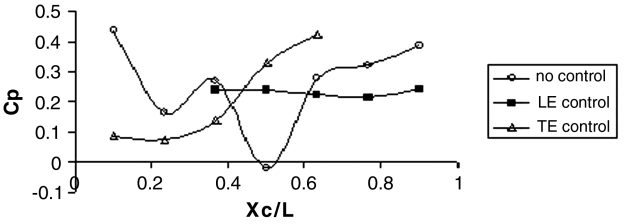

Fig. 9 Pressure distributions for cavity $L/D = 6$ with 30° wedge on leading or trailing edge.

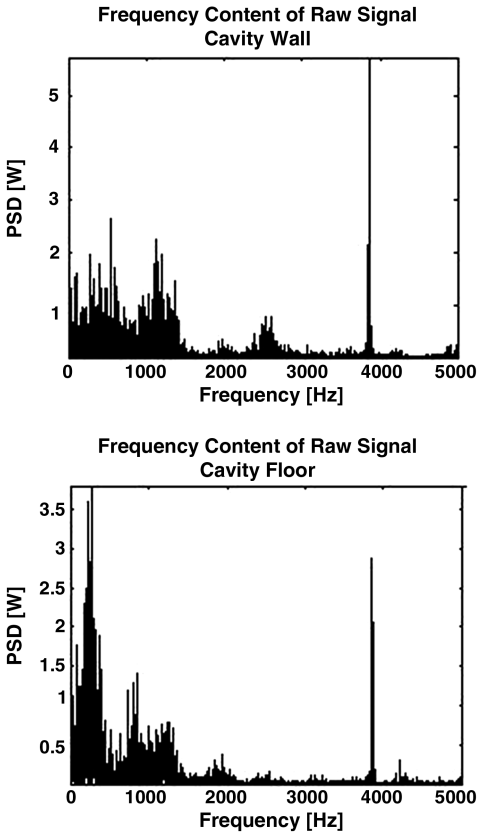

Fig. 7 Frequency content for cavity $L/D = 6$ with 15° wedge located at the leading edge.

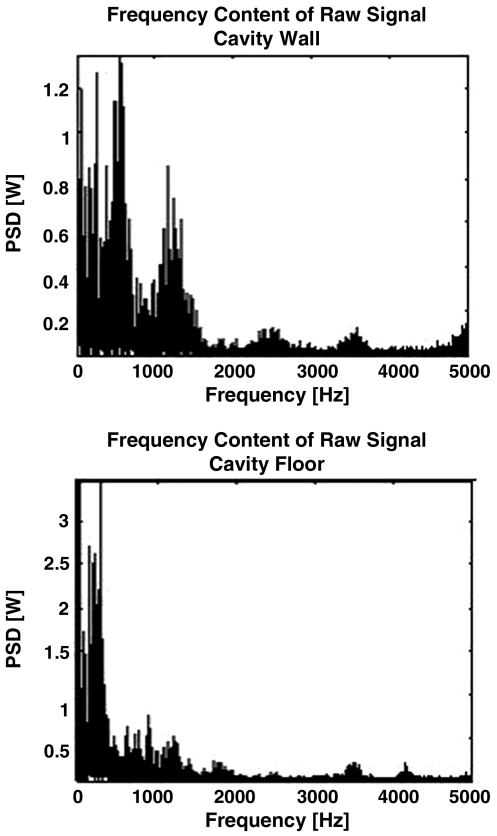

Fig. 10 Frequency content for cavity $L/D = 6$ with 30° wedge located at the leading edge.

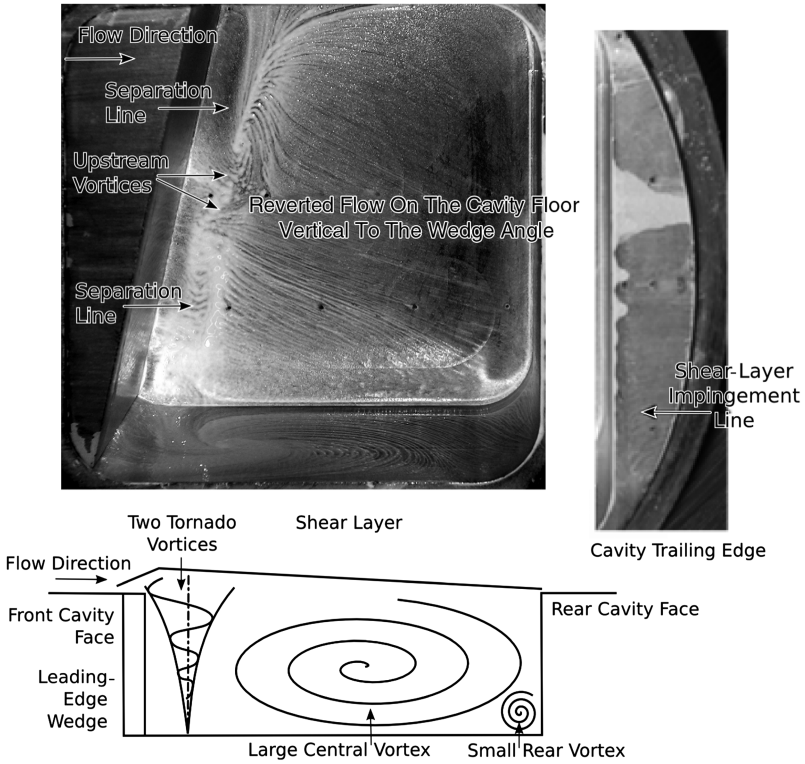

Fig. 11 Oil flow visualization for cavity $L/D = 2$, with 15° wedge placed at the leading edge, and schematic of the cavity side-view flow.

on the wedge, slightly higher pressure levels are recorded (Fig. 4) compared with the no-control case. The shear-layer trailing-edge impingement follows the shape of the tilted trailing edge. This means that the shear layer does not impinge on the trailing edge simultaneously, and the sound waves caused by the impingement are not as strong as the straight trailing-edge case.

By tilting the cavity leading edge 30°, large reductions in PSD across all modes were achieved, and the feedback loop is disrupted,

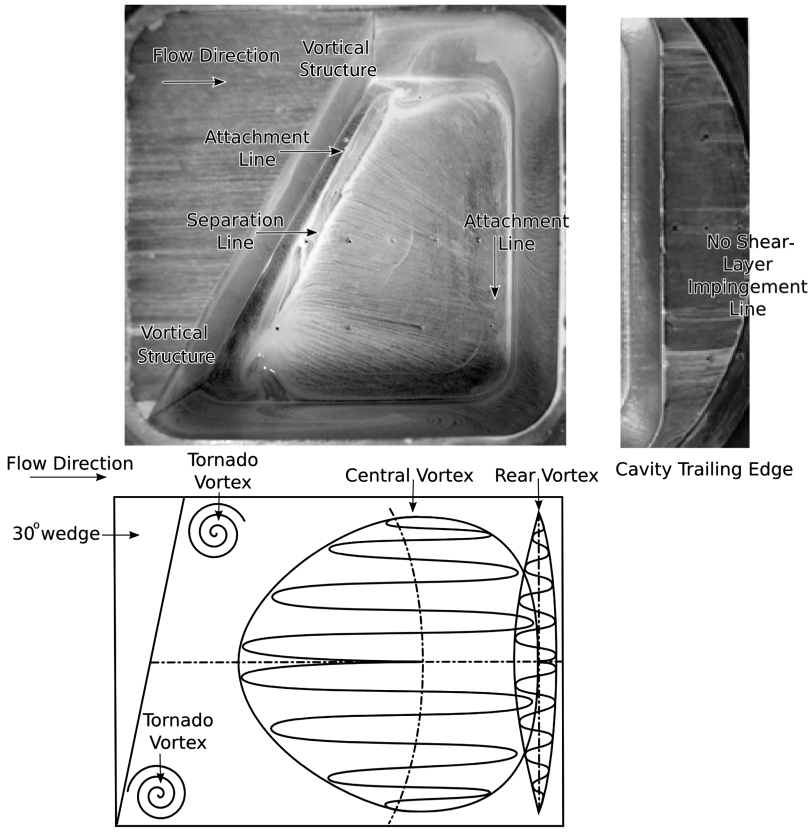

Fig. 12 Oil flow visualization for cavity $L/D = 2$, with 30° wedge placed at the leading edge, and schematic of the cavity plan-view flow.

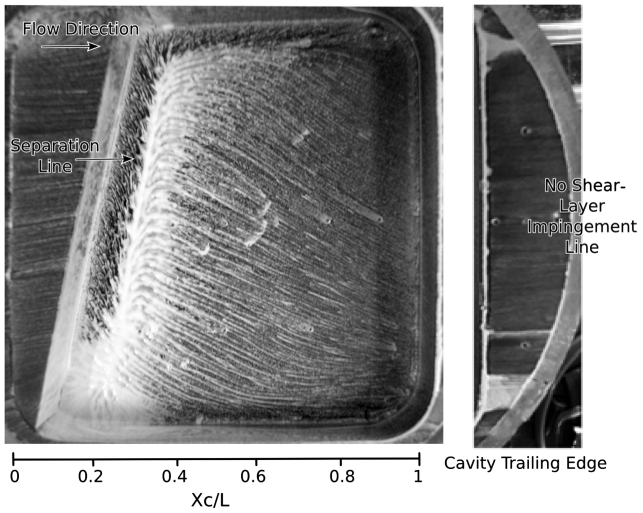

Fig. 13 Oil flow visualization for cavity $L/D = 6$, with 15° wedge placed at the leading edge.

because the shear layer is forced to impinge further downstream than the cavity trailing edge. The pressure measurements for the 30° wedge placed at the cavity leading edge (Fig. 6) indicate a reduction of pressure at the cavity trailing edge and a more uniform pressure distribution throughout the cavity floor. The cavity still behaves as an open cavity, which means that the acoustic suppression is achieved because the feedback loop is disrupted and not because the L/D ratio is altered by the bigger wedge. Placing the 30° wedge at the trailing edge of the cavity produced a shift in modal frequencies from 2500 to 1500 Hz, and the power of this mode, which is also the dominant one, was greatly attenuated down to 1.2 W. The fourth peak occurring at 4900 Hz has been completely attenuated. The static pressure measurements showed a higher pressure drop at the trailing edge, compared with the leading-edge wedge and the no-control cases (Fig. 6). When the 45° wedge was placed at the cavity leading or trailing edge, the pressure distribution showed that the L/D was greatly affected and the cavity behaved as transitional. This means that no acoustic tones were present any more; however, the available space was greatly reduced. The 60° wedge covered more than half of the cavity storage volume, and erroneous conclusions were derived from the experimental results due to lack of pressure tapings.

The main effect of the 15° wedge placed at the leading edge of the $L/D = 6$ cavity is that the second mode at 1750 Hz has been attenuated and there is a frequency shift toward the lower end of the spectrum (Fig. 7). The pressure distribution shown in Fig. 8 indicates that the flowfield is closer to transitional than to open. When the 15° wedge was placed at the trailing edge of the $L/D = 6$ cavity, only two significant modes were generated. Mode 2 was completely attenuated. The third mode compared with the no-control case was shifted to 3800 Hz and had no reduction in PSD, and mode 1 had been obtained. The pressure distribution indicated similar results to the leading-edge case.

The unsteady pressure measurements show a significant reduction in the PSD for all modes and locations (Fig. 9) when the 30° wedge was placed at the cavity leading edge. Modes 2 and 3, which are the most dominant modes, were totally attenuated. The pressure distribution shows an open cavity flowfield (Fig. 10). The amount of pressure dissipated at the cavity leading edge is reduced. Acoustic suppression is possible for that case. By placing the 30° wedge at the trailing edge of the cavity, the flowfield changed from open to transitional (Fig. 10). The results revealed large reductions in PSD across all modes for this configuration. This was an expected effect, since transitional cavities do not suffer from acoustic oscillations.

Figures 11 and 12 show the oil flow results obtained when the 15 or 30° wedge was inserted in the $L/D = 2$ cavity, respectively. The two tornado vortices rotate on the opposite direction compared with the counter-rotating direction observed for the no-control case. The pressure distribution results indicated only one circulating region, which is in good agreement with the oil flow results. The unsteady pressure measurements indicated an increase of cavity tones for the 15° wedge case. By comparing the shear layer impingement locations in Figs. 11 and 12, it becomes clear that the 30° wedge disrupted the feedback loop in such a way that the shear layer impinges further downstream of the cavity trailing edge since no line of attachment is present anymore. The flow appears to be attached throughout the whole trailing-edge region. Figure 13 shows the oil flow results obtained when the 15° wedge was inserted in the $L/D = 6$ cavity. A recirculation flow is observed over the cavity floor: movement of flow from the high-pressure region at the trailing region to the low-pressure region at the leading edge. No vertical structures are observed for the $L/D = 6$ cavity. A separation line just aft of the cavity leading edge parallel to the wedge is common for all cases. Again, no shear-layer impingement line is observed at the cavity trailing edge, which means that the wedge forced the shear layer to impinge further downstream, and the feedback loop was disrupted. Similar results were observed when the 30° wedge was inserted in the $L/D = 6$ cavity.

IV. Conclusions

The greatest attenuation for cavity $L/D = 2$ was achieved when the 30° wedge was placed at the trailing edge. For that case, the pressure measurements showed that the cavity flowfield was still open and the reason that the tones of the cavity were suppressed was because the shear layer was disturbed. For cavity $L/D = 6$, the pressure measurements indicated that the flowfield changed from open to transitional as soon as the 15° wedge was placed inside the cavity. Acoustic attenuation was achieved for that case too, but only because the L/D ratio of the cavity was affected by the wedge.

References

[1] Roshko, A., "Some Measurements of Flow in a Rectangular Cutout," NACA TN 3488, 1955.

[2] Krishnamurty, K., "Acoustic Radiation from Two Dimensional Rectangular Cutouts in Aerodynamic Surfaces," NACA TN 3487, 1955.

[3] Rossiter, J. E., "Wind-Tunnel Experiments on the Flow Over Rectangular Cavities at Subsonic and Transonic Speeds," British Aeronautical Research Council Reports and Memoranda 3438, London, 1964.

[4] Sarohia, V., "Experimental Investigation of Oscillations in Flows Over Shallow Cavities," *AIAA Journal*, Vol. 15, No. 7, 1977, pp. 984–991. doi:10.2514/3.60739

[5] Plentovich, E. B., Stallings, R. L., and Tracy, M. B., "Experimental Cavity Pressure Measurements at Subsonic and Transonic Speeds," NASA TP 3669, 1993.

[6] Tracy, B. M., and Plentovich, B. E., "Cavity Unsteady-Pressure Measurements at Subsonic and Transonic Speeds," NASA TP 3669, 1997.

[7] Perng, W. S., and Dolling, D. S., "Attenuation of Pressure Oscillations in High Speed Cavity Flow through Geometry Changes," AIAA Paper 1997-1802, 1997.

[8] Anavaradham, T. K. G., Babu, V., Chandru, U. B., Chakravarthy, R. S., and Panneerselvam, S., "Experimental and Numerical Investigations of Confined Unsteady Supersonic Flow Over Cavities," AIAA Paper 2002-2405, 2002.

[9] Hamed, A., Basu, D., and Das, K., "Detached Eddy Simulations of Supersonic Flow over Cavity," AIAA Paper 2003-0549, 2003.

[10] Sahoo, D., Annaswamy, A., Zhuang, N., and Alvi, F., "Control of Cavity Tones in Supersonic Flow," AIAA Paper 2005-0793, 2005.

[11] Plentovich, E. B., "Study of Three-Dimensional Cavity Flow at Transonic Speeds," AIAA Paper 1988-2032, 1988.

[12] Wood, M. R., Wilcox, J. F., Bauer, X. S. S., and Allen, M. J., "Vortex Flows at Supersonic Speeds," NASA TP 211950, 2003.

[13] Zhang, X., Rona, A., and Edwards, A. J., "An Observation of Pressure Waves Around a Shallow Cavity," *Journal of Sound and Vibration*, Vol. 214, No. 4, 1998, pp. 771–778. doi:10.1006/jsvi.1998.1635

[14] Chung, K. M., "Characteristics of Transonic Rectangular Cavity Flows," *Journal of Aircraft*, Vol. 37, No. 3, 2000, pp. 463–468. doi:10.2514/2.2620

[15] Maull, D. J., and East, L. F., "Three-Dimensional Flow in Cavities,"

Journal of Fluid Mechanics, Vol. 16, No. 4, 1963, pp. 620–632. doi:10.1017/S0022112063001014

[16] Heller, H. H., Holmes, D. G., and Covert, E. E., "Flow Induced Pressure Oscillations in Shallow Cavities," *Journal of Sound and Vibration*, Vol. 18, No. 4, 1971, p. 545. doi:10.1016/0022-460X(71)90105-2

[17] Colonius, T., "An Overview of Simulation, Modelling, and Active Control of Flow/Acoustic Resonance in Open Cavities," AIAA Paper 2001-0076, 2001.

[18] Cattafesta, L., Williams, D., Rowley, C., and Alvi, F., "Review of Active Control of Flow Induced Cavity Resonance," AIAA Paper 2003-3567, 2003.